

Lattice Dynamics of Silver Chloride*

P. R. Vijayaraghavan,[†] R. M. Nicklow, H. G. Smith, and M. K. Wilkinson
Solid State Division, Oak Ridge National Laboratory, Oak Ridge, Tennessee 37830

(Received 12 February 1970)

The dispersion relation for the normal modes of vibration in AgCl at 78 °K has been determined from neutron coherent inelastic scattering data obtained on a triple-axis neutron spectrometer at the Oak Ridge High Flux Isotope Reactor. Some difficulty in obtaining a satisfactory fit to the results with a simple shell model was encountered. Only a fair fit to the data is obtained with an 11-parameter model, which includes next-nearest-neighbor interactions for both types of ions, a variable ionic charge, and the electrical and mechanical polarizabilities for both ions. A 13-parameter model, while providing an improved fit to the data, gives values for several of the parameters that have no obvious physical significance. The neutron data are in reasonably good agreement with the results of low-temperature measurements of the elastic constants and the infrared absorption. A frequency-distribution function has been computed, together with the lattice heat capacity and the mean-square displacements for each ion. A combined density-of-states function has also been obtained for comparison with the relevant optical data.

I. INTRODUCTION

The lattice dynamics of ionic crystals with the sodium chloride type of structure has been both theoretically and experimentally investigated by several authors. The point-ion model developed by Kellermann¹ has been modified to take into account the polarizabilities of both ions.²⁻⁵ This shell model, which takes into account the short-range overlap forces, the long-range Coulomb interactions, and the ionic polarizabilities, has been found quite adequate to interpret the phonon spectrum in several solids where the departure from the Cauchy relation ($C_{12} = C_{44}$) is not too severe. In such solids the forces are expected to be central and two body in character.

One of the primary aims of the present work was to investigate the applicability of the shell model, with the usual simplifying restrictions,^{4,5} to AgCl. Although silver chloride has the sodium chloride structure, it is partially covalent because the outer electrons of Ag^+ do not form a closed-shell configuration. This probably leads to the unusual elastic behavior of this material which has been found to exhibit a very large departure from the Cauchy relation; C_{12} is approximately 5 times larger than C_{44} . It has also been observed that the shell model gives less satisfactory results for crystals with high values of the high-frequency dielectric constant, ϵ_{∞} .⁶ The value of this constant for AgCl is 4.04, which is about 50% higher than that for many of the alkali halides.

It was also of interest to investigate how well a harmonic theory can describe the lattice dynamics of a solid like silver chloride, which has several properties suggestive of a high degree of anharmonicity. For example, there is a 28% increase in the value of the C_{11} elastic constant between 300 and 0 °K,⁷ and optical measurements⁸⁻¹⁰ on the

$q = 0$ transverse optic mode show a large temperature dependence for the frequency of this mode. In addition to the optical measurements for $q = 0$, frequencies for normal modes at selected points in the Brillouin zone of AgCl have been predicted from data based on indirect optical transitions.^{11,12}

Unlike optical processes, neutron scattering techniques allow observation of one-phonon scattering processes at any point in the Brillouin zone; hence, they are capable of continuous mapping of the dispersion relation connecting the frequency of a normal mode of vibration of the crystal lattice to its wave vector. Such information should help correlate all existing data pertaining to the lattice dynamics of AgCl on the basis of a more fundamental theory. In this paper we report neutron scattering measurements of the phonon dispersion relation of AgCl at liquid-nitrogen temperature (78 °K), along with a few measurements at room temperature.

II. EXPERIMENT AND RESULTS

A. Sample

The sample used in the experiment was a single crystal supplied by Childs and Slifkin of the University of North Carolina. Special precautions were taken to avoid any contamination of the sample owing to chemical reactions with the holder. The crystal had dimensions of $0.5 \times 0.5 \times 1.8$ in., and the mosaic spread was approximately 0.2° . It was oriented with the $[1\bar{1}0]$ axis vertical so that measurements along the three principal high-symmetry directions could be made without remounting the sample.

B. Theoretical Basis and Experiment

It is well known that when a beam of monochromatic neutrons is scattered from a single-crystal specimen, the scattering can be either elastic or

inelastic. In inelastic scattering due to atomic vibrations, the energy of the scattered neutron is different from its initial energy because a phonon has been created or annihilated. The following conservation conditions apply in the case of the one-phonon inelastic scattering:

$$\vec{k}_0 - \vec{k}' = \vec{Q} = 2\pi\vec{\tau} + \vec{q}, \quad (1)$$

$$E_0 - E' = \pm \hbar\nu. \quad (2)$$

The symbols have the usual meaning,¹³ and $\nu = \nu_j(\vec{q})$ represents the dispersion relation for the normal modes of vibration in the crystal. Well-defined peaks should occur when both of the above conditions are satisfied. The differential cross section per primitive unit cell, for scattering by phonons of the type $\nu_j(\vec{q})$, is given for the "constant Q " mode of operation by¹³⁻¹⁵

$$\sigma_j(\vec{k}_0 \rightarrow \vec{k}') = \frac{\hbar}{4\pi k_0} \left\{ \frac{N_j}{N_j + 1} \right\} e^{-2W} g_j^2(\vec{q}, \vec{\tau}), \quad (3)$$

where $N_j = (e^{\hbar\nu_j/kT} - 1)^{-1}$. The population factor N_j is used in cases of phonon annihilation and $N_j + 1$ is used for phonon creation; e^{-2W} is the Debye-Waller factor; and $g_j^2(\vec{q}, \vec{\tau})$ is the dynamical structure factor. The latter is given by¹⁴

$$g_j^2(\vec{q}, \vec{\tau}) = \left| \sum_k (b_k \vec{Q} \cdot \vec{\xi}_{jk}(\vec{q}) / [M_k \nu_j(\vec{q})]^{1/2}) e^{i\vec{Q} \cdot \vec{r}(k)} \right|^2. \quad (4)$$

Here the summation k is over the atoms in the unit cell and $\vec{r}(k)$ is the position vector of the k th atom; $\vec{\xi}_{jk}(\vec{q})$ is the polarization vector; and b_k is the bound scattering amplitude of the atom k whose mass is M_k . This expression can be simplified for \vec{q} lying along a symmetry direction and the simplified expression is given in Sec. III.

Preliminary experiments were initiated at the Oak Ridge Research Reactor (ORR) HN-4 triple-axis facility.¹⁶ The "constant Q " mode of operation was employed throughout and the experimental conditions were such that phonon creation processes were observable. The data at the ORR facility consisted mainly of measurements of phonons having transverse polarization and only a few having longitudinal polarization were observed. These data, together with reported optical measurements, were used to generate the parameters for a preliminary shell model which was used to calculate the dispersion relation. Preliminary structure factor calculations, based on the approximate model, were also used as a guide to select appropriate regions in reciprocal space where suitable intensities could be expected. A complete mapping of the dispersion relation was rendered extremely difficult at the ORR facility because of the high absorption ($\sim 30-50 b$) of the crystal and because of the relatively low structure factor for parts of several branches. However, these preliminary data provided a basis for continuing the measurements along the [100], [110], and [111] high-symmetry directions, using the computer-controlled HB-3 triple-axis spectrometer¹⁷ at the Oak Ridge High Flux Isotope Reactor.

The sample was kept at liquid-nitrogen temperature in a cryostat. Helium gas at a very low pressure surrounded the sample to assure uniformity of temperature across the sample.

C. Results

The measured dispersion relation for phonons propagating along the [100], [110], and [111] directions is shown in Fig. 1. The labeling of the

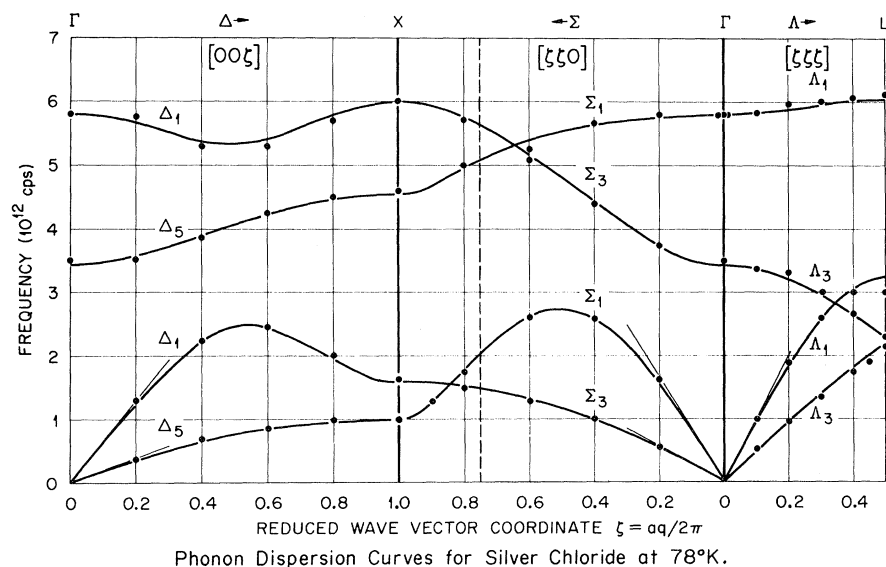


FIG. 1. Experimental dispersion curves along the three high-symmetry directions of silver chloride at 78°K. The solid lines are the best least-squares fit to the results on the basis of a 13-parameter shell model. The straight lines through the origin represent the dispersion curve slopes as deduced from the measured elastic constants (Ref. 7).

branches is consistent with the notation used by Koster.¹⁸ The experimental errors are generally of the order of 2%, and no corrections have been applied for the large absorption in the sample. The continuous lines correspond to fitted curves based on a 13-parameter shell model which is discussed in Sec. III. The frequencies of the longitudinal optic and transverse optic modes at $q=0$ have been measured with great care in order to check the validity of the Lyddane-Sachs-Teller relation.¹⁹ No measurements have been attempted on the transverse branch along Σ which is polarized in the $[1\bar{1}0]$ direction. The acoustic branches also have been measured at room temperature for comparison with the available x-ray data,²⁰ and these data are discussed briefly in Sec. IV.

III. THEORETICAL CALCULATIONS

A. Models

The dynamics of crystal lattices with the sodium chloride structure has been investigated in detail by Kellermann,¹ who used a point-ion model which took into account long-range electrostatic and arbitrary short-range overlap forces. The equation of motion in this framework can be written as

$$\vec{M}\omega^2\vec{u} = (\vec{R} + Z\vec{C}Z)\vec{u}, \quad (5)$$

where \vec{M} is a matrix containing masses of ions, \vec{u} is a vector containing the ionic displacements from their equilibrium positions, \vec{R} is a matrix specifying the short-range interactions, and \vec{C} is a matrix of dimensionless Coulomb coefficients. This model, however, does not take into account the polarizability of the ions, and hence does not include the electrostatic forces arising from the distortions of the ions due to the lattice waves. The shell-model concept was introduced by Dick and Overhauser,² and Henlon and Lawson³ to take into account these distortions, and the model has been extended by Woods, Cochran, and Brockhouse⁵ to calculate phonon frequencies in several alkali halides. In the framework of the shell model developed by Cochran *et al.*,⁶ the equations of motion can be expressed as

$$\vec{M}\omega^2\vec{u} = (\vec{R} + Z\vec{C}Z)\vec{u} + (\vec{T} + Z\vec{C}Y)\vec{W}, \quad (6)$$

$$0 = (\vec{T} + Y\vec{C}Z)\vec{u} + (\vec{S} + Y\vec{C}Y)\vec{W}, \quad (7)$$

where \vec{R} , \vec{T} , and \vec{S} are matrices which describe the short-range core-core, core-shell, and shell-shell interactions, respectively, Y is the charge on the shell, and \vec{W} is a vector defined such that $Y\vec{W}$ is dipole moment of the ion.²¹ The most generalized shell model, which includes second-neighbor interactions, has 29 adjustable parameters. However, the number is reduced to 12 by restricting

the model to be axially symmetric and setting $\vec{R} = \vec{T}$ and $\vec{S} = \gamma_s\vec{R}$ (where γ_s is an arbitrary constant) for all wave vectors. If one relaxes the condition $\vec{R} = \vec{T}$ to allow near-neighbor core-shell interactions, then two additional parameters $\beta_T(21)$ and $\beta_T(12)$ are introduced as discussed by Cochran *et al.*⁶

The neutron data, together with the elastic constants and the high-frequency dielectric constant, have been used to generate various models by the method of nonlinear least squares. The best-fitted model has 13 adjustable parameters and restricts $\gamma_s = 1$. The parameters are A, B, A', B', A'', B'' , for the short-range radial and tangential force constants between near neighbors, second-nearest-neighbor positive ions and second-nearest-neighbor negative ions, respectively; Ze , the ionic charge; and $\alpha_1, d_1, \alpha_2, d_2$ the electrical and mechanical polarizabilities of the positive and negative ions, respectively. Two additional parameters $\beta_T(12)$ and $\beta_T(21)$ have already been mentioned.

The parameters as obtained from the least-squares analysis are given in Table I. The quality of the fit of a model to the measurements is characterized by the standard error χ . It is approximately a measure of the average ratio of the deviation of the fit to the experimental error.

Model I includes the polarizability of chlorine ions and $\text{Cl}^- - \text{Cl}^-$ interactions. It does not give a good fit to the $\Delta_5(\text{TO})$ and $\Sigma_1(\text{LO})$ branches and to the value of the high-frequency dielectric constant.

In model II the second-neighbor positive-ion interactions and positive-ion polarizabilities are included. These additions considerably improve the fit to the data, but the model predicts a very low value for ϵ_∞ and α_1 . Relaxing the condition that $\gamma_s = 1$ in the equation $\vec{S} = \gamma_s\vec{R}$ in this particular model did not improve the fit significantly. Hence γ_s was set equal to 1 in the subsequent calculations.

TABLE I. Parameters for the four shell models for silver chloride discussed in text (v is the volume of the primitive unit cell).

Parameter	Unit	I	II	III	IV
A	$(e^2/2v)$	10.880	13.720	11.370	9.050
B	$(e^2/2v)$	-1.440	-2.570	-1.450	-1.810
A'	$(e^2/2v)$...	-1.470	-0.530	-0.026
B'	$(e^2/2v)$...	0.440	0.150	0.025
A''	$(e^2/2v)$	2.300	2.240	1.850	2.200
B''	$(e^2/2v)$	-0.800	-0.720	-0.700	-0.280
Z	(e)	0.930	1.140	0.960	0.850
α_1	$(1/v)$...	0.000	0.000	0.000
d_1	(e)	...	0.002	-0.006	-0.017
α_2	$(1/v)$	0.084	0.087	0.130	0.120
d_2	(e)	0.177	0.319	0.217	0.058
$\beta_T(12)$...	1.000	1.000	3.850	4.440
$\beta_T(21)$...	1.000	1.000	1.000	-0.660
χ	...	4.920	3.200	2.530	2.070

Models III and IV include the near-neighbor core-shell forces which are nonsymmetric. In model III, $\beta_T(21)$ is set = 1, whereas in model IV this restriction is relaxed. The frequencies calculated with model IV, which gives the best fit to the data, are shown in Fig. 1 as the continuous curve through the data points.

Although model IV gives the best fit to the data, the fit is not very good, particularly when compared to that obtained for many of the alkali halides.⁵ In addition the negative signs of $\beta_T(21)$ and d_1 are physically unreasonable. The measured crystal polarizability²¹ is, however, in quite good agreement with the sum of α_1 and α_2 . The deficiencies of these models indicate that the simple shell model does not provide a truly satisfactory description of the lattice dynamics of AgCl and that one cannot attach too much physical significance to the parameters. Future work on more complicated models is certainly desirable, but it is believed that model IV can provide a useful basis for the calculation of many quantities related to the dynamical properties of AgCl.

B. Calculations Based on Model IV

Using the notation in Sec. II, the inelastic struc-

ture factor for \vec{q} along a symmetry direction can be written as

$$g_j^2(\vec{q}, \vec{\tau}) = \frac{(\xi_j \cdot \vec{Q})^2}{\nu_j} \frac{b_2^2}{M_2} \frac{[(b_1/b_2) \pm U_j(2)/U_j(1)]^2}{(M_1/M_2) \pm [U_j(2)/U_j(1)]^2}, \quad (8)$$

where $U_j(k) = |\xi_{jk}|/\sqrt{M_k}$, b_1 and b_2 are the bound coherent scattering amplitudes, M_1 and M_2 are the masses of the two ions, and ξ_j is a unit vector in the direction of polarization. The Debye-Waller factor has been assumed to be the same for both types of ions. The plus and minus signs correspond to reciprocal-lattice vectors having even and odd indices, respectively. The results of such a calculation are shown in Fig. 2 in units of $(\xi_j \cdot \vec{Q} b_2)^2/\nu_j M_2$. It is noted that the longitudinal acoustic branches have in general very low structure factors.

A frequency distribution function $g(\nu)$, based on the Gilat-Raubenheimer²² approach, has also been calculated and is shown in Fig. 3. This distribution function has been used to calculate the specific heat and associated Debye temperature in the harmonic approximation as a function of temperature. The comparison of the calculated θ_D with that obtained from calorimetric measurements by Eastman and Milner²³ and by Berg²⁴ is shown in

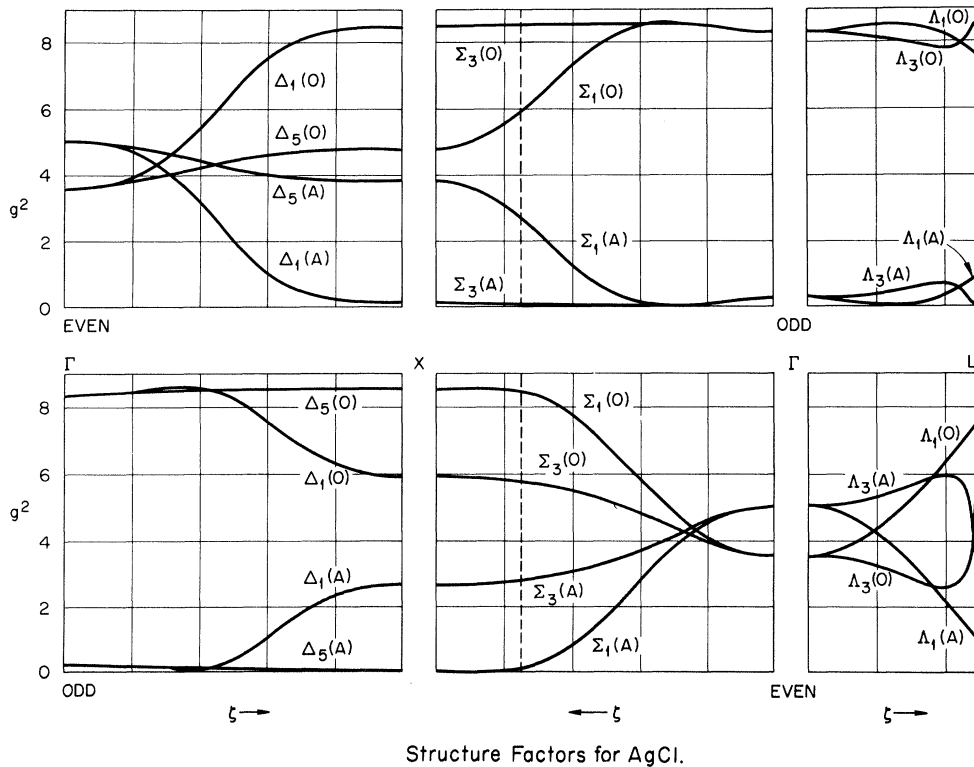


FIG. 2. Inelastic scattering structure factors for silver chloride, calculated on the basis of model IV and plotted in units of $(\xi_j \cdot \vec{Q} b_2)^2/\nu_j M_2$.

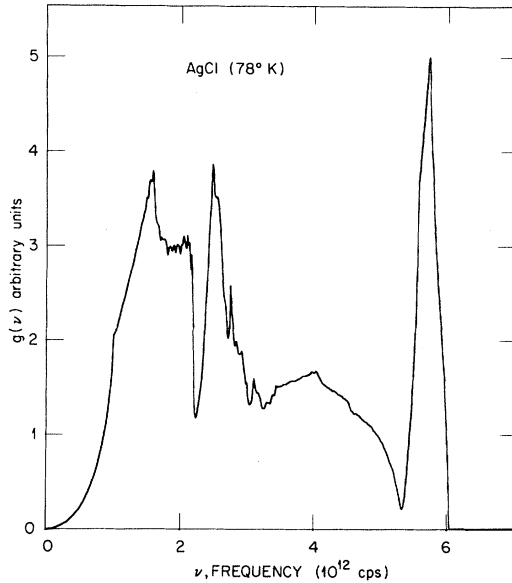


FIG. 3. Frequency distribution function for phonons in silver chloride calculated with model IV.

Fig. 4. Throughout most of this temperature region the calculated curve is somewhat higher than the measured values. This probably is due to the limitations of the 13-parameter model. The low-temperature limit of θ_D agrees fairly well with the values obtained from calorimetry and elastic constant measurements.

The mean-square displacements for the Ag^+ and Cl^- ions have also been computed. The method used is that described by Dolling *et al.* for Li^7F ,¹⁶ whereby a distribution function, weighted by the appropriate polarization vectors, is constructed for each ion. The results of these calculations are shown in Fig. 5. It is interesting that above 100°K the heavier ion has the larger mean-square displacement, which is a result that is consistent with x-ray measurements of the Debye-Waller factors for AgCl .²⁵

IV. DISCUSSION

The measured values of the frequencies of the $q=0$ transverse optic and longitudinal optic modes are 3.50 ± 0.03 (10^{12} cps) and 5.80 ± 0.06 (10^{12} cps) which give a value of 1.66 ± 0.03 for the ratio $\nu(\text{LO})/\nu(\text{TO})$. These two frequencies are, however, related by the Lyddane-Sachs-Teller (LST) relation¹⁹ to the static and high-frequency dielectric constants according to the formula

$$\epsilon_0/\epsilon_\infty = [\nu_L(q \rightarrow 0)/\nu_T(q \rightarrow 0)]^2. \quad (9)$$

The value of ϵ_0 at 78°K is not available; however, a value at 90°K has been reported by Lowndes.²⁶ Using his value of 9.92 for ϵ_0 , the result for $(\epsilon_0/$

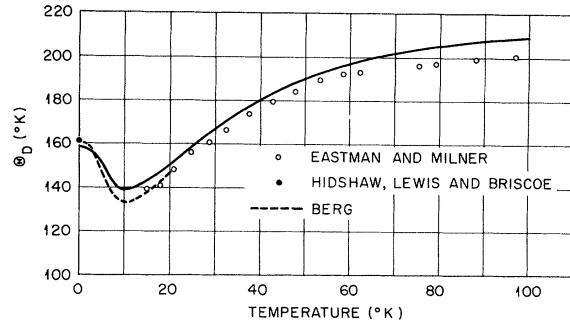


FIG. 4. Variation of the Debye temperature of AgCl as derived from neutron scattering measurements, calorimetric data, and elastic constants.

$\epsilon_\infty)^{1/2}$ is determined to be 1.57. This number is sufficiently different from the neutron measurement to tentatively conclude that the LST relation is not valid, because the quoted error for ϵ_0 is only 1%. On the other hand, the values of ϵ_0 measured at room temperature (see Table II) by various experimenters show that at present this constant has a 10% uncertainty. This leads to a 5% uncertainty in $(\epsilon_0/\epsilon_\infty)^{1/2}$, and thus precludes a rigorous verification of the LST relation.

To examine the influence of anharmonicity on the dispersion relation of AgCl , measurements at different temperatures are required. These measurements have not been completed; however, some data for the acoustic branches have been obtained at room temperature. The average change

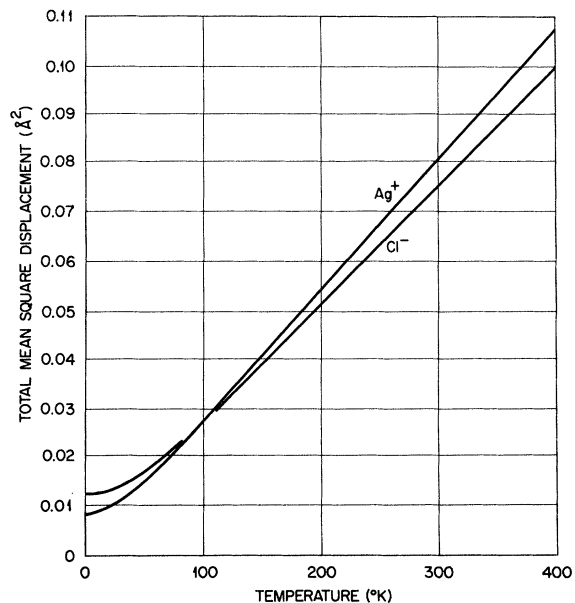


FIG. 5. Mean-square ionic displacements for silver and chlorine ions.

TABLE II. Static dielectric constant of AgCl.

(300 °K)	(90 °K)	Frequency (cps)	Reference
11.2	...	10^2-10^7	a
12.6	...	10^{12}	b
12.3	...	3×10^6	c
10.9	...	$\sim 10^8$	d
14.1	...	?	e
$\sim 12.6 \pm 0.4$...	?	f
13.0	...	?	g
11.15 ± 0.08	9.92 ± 0.1	10^2-10^6	h
12.7	...	?	i

^aR. Jaeger, *Ann. Physik*, **53**, 409 (1917).

^bT. Leisbisch and H. Rubers, *Ber. Berl. Akad.* **876** (1919); **211** (1921).

^cA. Eucken and A. Buchner, *Z. Physik. Chem.* **27B**, 321 (1934).

^dA. Heydweiller, *Z. Physik* **3**, 308 (1920).

^eN. V. Sathe *et al.*, *J. Indian Chem. Soc.* **22**, 29 (1945).

^fG. C. Smith, thesis, Cornell University, 1962 (unpublished), Fig. 16.

^gK. L. Kliewer, *J. Phys. Chem. Solids* **27**, 705 (1966) (Eq. 20 on p. 707).

^hR. P. Lowndes, *Phys. Letters* **21**, 26 (1966).

ⁱR. W. Tyler (private communication).

in frequency for these modes between 78 and 298 °K is observed to be a reduction of approximately 9%. Our room-temperature results are compared to the x-ray measurements of Cole¹⁹ in Fig. 6. Except for the $TA[\xi 00]$ branch, the x-ray results generally fall significantly below the neutron measurements, particularly at the $[\xi \xi \xi]$ zone boundary. Such discrepancies are probably due to Cole's underestimate of the corrections for the x-ray scattering contribution from the optic branches. The shapes of these branches are quite different from those assumed by Cole, particularly near the $[\xi \xi \xi]$ zone boundary.

Brandt¹⁰ has determined the frequencies of the LO and TO modes at zero wave vector by measuring the optical transmission of thin films. The values obtained at 9.3 °K are 5.91 and 3.66 (units of 10^{12} cps), respectively. Room-temperature optical measurements⁸ give 5.43 and 3.09 (10^{12} cps), respectively, for the frequencies of these modes. A linear interpolation between these high-temperature and low-temperature optical measurements is in excellent agreement with the neutron scattering results quoted earlier. The assignment given by Bottger⁹ for the absorption bands in AgCl at 143 °K in the far-infrared region due to combination bands is also consistent with the neutron measurements. The modes participating in these transitions can be identified as the acoustic and transverse optic modes at the $[111]$ zone boundary.

A combined density of states has been calculated for AgCl by the method described by Dolling *et*

*al.*¹⁶ and is shown in Fig. 7. At each \vec{q} in the Brillouin zone, each of the six normal-mode frequencies is added to the other frequencies in turn (including itself) and the resultant two-phonon sum frequencies are sorted into a histogram. The points labeled A and B in Fig. 7 correspond to the sum frequencies observed by Bottger.⁹ It is hoped that this calculation will stimulate further investigation of the second-order spectra of AgCl by optical methods.

Bassani, Knox, and Fowler¹¹ have interpreted certain structure in the optical absorption edge of AgCl on the basis of phonon-assisted indirect electronic transitions. For example, they have suggested that the transition from the energy maxi-

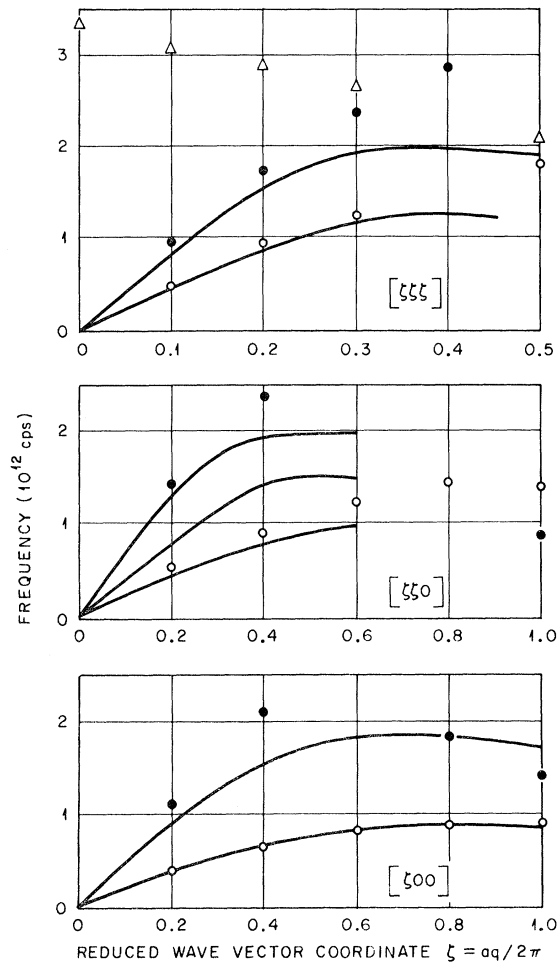


FIG. 6. Comparison of the neutron room-temperature data for the dispersion relation of the acoustic branches in AgCl with the x-ray measurements of Cole. The continuous curves are the x-ray measurements. Neutron measurements: triangle represents transverse optic modes; solid circle represents longitudinal acoustic modes; open circle represents transverse acoustic modes.

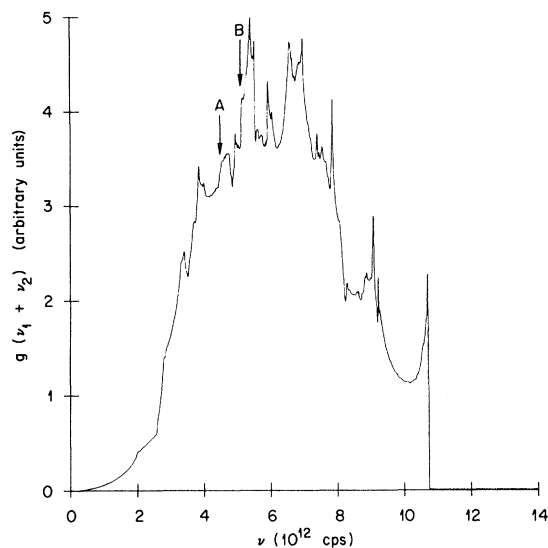


FIG. 7. Combined density-of-states function for AgCl at 78°K. Only summation bands and combination bands are included. The arrows indicate certain sum frequencies observed in the infrared absorption of AgCl at 143°K (see Ref. 10).

mum in their calculated valence band at the point L (see Fig. 1) to the minimum in the conduction band at the point Γ ($L'_3 \rightarrow \Gamma_1$ according to their notation) is assisted by a longitudinal acoustic phonon at L with an energy corresponding to 93°K (a frequency of about 1.94×10^{12} cps). This particular phonon was specified because it possesses the correct symmetry properties²⁷ and, according to the x-ray measurements of Cole,²⁰ it appeared to have the appropriate frequency. However, it is seen from our results that this phonon has a frequency of 3×10^{12} cps which is about 50% higher than that reported by Cole. On the other hand, both the transverse acoustic and the transverse optic phonons at the point L have approximately the right frequency required for the transition.

V. SUMMARY

The results presented here show that the simple shell model does not provide a completely satisfactory description of the lattice dynamics

of AgCl. The 7-to-11-parameter models that were calculated give a substantially poorer fit to the measured phonon dispersion relation for AgCl than similar models obtained for many alkali halides.^{4,5,16} The 13-parameter model, while providing an improved fit to the data, gives values for several of the parameters that have no obvious physical significance.

The best-fitted 13-parameter model has been used to calculate various thermodynamical properties of AgCl. The calculated θ_D agrees with low-temperature measurements^{23,24} within about 3%. The calculated mean-square vibrational amplitude of Ag^+ is larger than that of Cl^- at temperatures above 100°K. This result is consistent with x-ray measurements of the Debye-Waller factor of AgCl.²⁵

The frequencies measured at $q \rightarrow 0$ and at various zone boundaries are in good agreement with those deduced from optical measurements. In particular, the frequencies measured at the $[111]$ zone boundary support the proposal that certain features observed in the fundamental optical absorption spectrum of AgCl are a result of indirect phonon-assisted electronic transitions.¹¹

The temperature dependence of the acoustic phonon frequencies is large. The average change in frequency measured between 78 and 298°K is a reduction of approximately 9%.

ACKNOWLEDGMENTS

The authors are indebted to Professor F. C. Brown for communicating low-temperature absorption data, and to Dr. G. L. Bottger for his observations on the static dielectric constant. One of us (P. R. V.) would like to express his appreciation to the U. S. Agency for International Development for the Fellowship he was granted, and to the Oak Ridge National Laboratory for the hospitality he enjoyed during his stay at Oak Ridge. The assistance of Charles Childs in obtaining the sample is gratefully acknowledged, and the use of computer programs developed by G. Dolling for various calculations is very much appreciated.

*Research sponsored by the U. S. Atomic Energy Commission under contract with Union Carbide Corp.

¹Present address: Nuclear Physics Division, Bhabha Atomic Research Centre, Bombay-85, India.

²E. W. Kellermann, Phil. Trans. Roy. Soc. London **A238**, 513 (1940).

³B. J. Dick and A. W. Overhauser, Phys. Rev. **112**, 90 (1958).

⁴J. E. Hanlon and A. W. Lawson, Phys. Rev. **113**,

472 (1959).

⁵W. Cochran, Phys. Rev. Letters, **2**, 495 (1959); Proc. Roy. Soc. (London) **A253**, 260 (1959).

⁶A. D. B. Woods, W. Cochran, and B. N. Brockhouse, Phys. Rev. **119**, 980 (1960).

⁷W. Cochran, R. A. Cowley, G. Dolling, and M. M. Elcombe, Proc. Roy. Soc. (London) **A293**, 433 (1966).

⁸W. Hidshaw, J. T. Lewis, and C. V. Briscoe, Phys. Rev. **163**, 876 (1967).

- ⁸G. O. Jones, D. H. Martin, P. A. Mawer, and C. H. Perry, Proc. Roy. Soc. (London) A261, 10 (1961).
- ⁹G. L. Bottger and A. L. Geddes, J. Chem. Phys. 46, 3000 (1967).
- ¹⁰F. C. Brown (private communication of Brandt's results).
- ¹¹F. Bassani, R. S. Knox, and W. B. Fowler, Phys. Rev. 137, A1217 (1965).
- ¹²F. C. Brown, T. Masumi, and H. H. Tippins, Phys. Chem. Solids 22, 101 (1961); see also F. C. Brown, J. Phys. Chem. 66, 2368 (1962).
- ¹³B. N. Brockhouse and P. K. Iyengar, Phys. Rev. 111, 747 (1958).
- ¹⁴I. Waller and P. O. Froman, Arkiv Fysik 4, 183 (1950).
- ¹⁵B. N. Brockhouse, *Inelastic Scattering of Neutrons in Solids and Liquids* (International Atomic Energy Agency, Vienna, 1961), p. 113.
- ¹⁶G. Dolling, H. G. Smith, R. M. Nicklow, P. R. Vijayaraghavan, and M. K. Wilkinson, Phys. Rev. 168, 970 (1968).
- ¹⁷M. K. Wilkinson, H. G. Smith, W. C. Koehler, R. M. Nicklow, and R. M. Moon, in *Neutron Inelastic Scattering* (International Atomic Energy Agency, Vienna, 1968), Vol. II, p. 253.
- ¹⁸G. F. Koster, in *Solid State Physics*, edited by F. Seitz and D. Turnbull (Academic, New York, 1957), Vol. V, p. 173.
- ¹⁹R. H. Lyddane, R. G. Sachs, and E. Teller, Phys. Rev. 59, 673 (1941).
- ²⁰H. Cole, J. Appl. Phys. 24, 482 (1953).
- ²¹W. Cochran, in *Advances in Physics*, edited by F. Mott (Taylor and Francis, London, 1961), Vol. 10, p. 401.
- ²²G. Gilat and L. J. Raubenheimer, Phys. Rev. 144, 390 (1966).
- ²³E. D. Eastman and R. T. Milner, J. Chem. Phys. 1, 444 (1933).
- ²⁴W. T. Berg (private communication).
- ²⁵R. M. Nicklow and R. A. Young, Technical Report No. 3, Office of Naval Research Contract No. NONR 991(00) and 991(06) (unpublished); NR-017-623, Georgia Institute of Technology, Atlanta, Georgia, Project A-389, 1964 (unpublished).
- ²⁶R. P. Lowndes, Phys. Letters 21, 26 (1966).
- ²⁷If Ag is at the origin, the symmetry is L'_2 ; if Cl is at the origin, the symmetry is L_1 .

Photon-Induced Reorientation of Color Centers

R. W. Dreyfus

IBM Thomas J. Watson Research Center, Yorktown Heights, New York 10598

(Received 29 December 1969)

The present experiment investigates the mechanism by which color centers reorient after the absorption of light. In the cases of M and F_A centers in alkali-halide crystals, the F -center portion of a center jumps to an adjacent lattice site after the center has absorbed a (~ 2 -eV) photon. From conventional optical measurements, Lüty deduced that the jumping occurs while the F center is in the relaxed excited state. To verify that the reorientation is indeed *not* due to a hot-spot type of phenomenon, the time dependence for the reorientation is measured. That is, the behavior of a color center is analyzed in terms of submicrosecond kinetics. To carry out this measurement, F_A centers are first oriented along a particular axis by illumination with polarized light in the F_{A2} absorption band. The centers are then excited, essentially instantaneously, by Q -switched ruby-laser light. From 0.1 to 10 μ sec after the laser flash, the number of centers oriented along each of the cubic axes is measured by the dichroic absorption of polarized F_{A2} light. Thus the reorientation process is followed for times comparable to the lifetime of the excited state. The dichroism of the KBr: F_A (Li) and RbCl: F_A (Na) systems is found to be time dependent. This result confirms the previous deduction that *reorientation occurs by thermally activated jumping* while the F_A center is in the relaxed excited state. An atypically low activation energy, ~ 0.06 eV, allows the jumping to occur rapidly even below 100°K. The present mechanism also explains the photon-induced reorientation of the M center.

I. INTRODUCTION

A number of color centers in alkali-halide crystals reorient¹ after absorbing an optical photon. Several centers possessing an identifiable axis become preferentially oriented after illumination with polarized light. The M center (which is a

pair of F centers on adjacent anion lattice sites) reorients because absorption of a photon stimulates the interchange of one of the F centers with a neighboring host halide ion. This behavior is not unique to the M center, and a general understanding of how a photon produces the interchange is desired.